GLACIER MASS BALANCE IN THE SOUTH-EASTERN SWISS ALPS SINCE 1900 AND PERSPECTIVES FOR THE FUTURE

Matthias Huss, Stephanie Usselmann,
Daniel Farinotti and Andreas Bauder

With 14 figures and 8 tables
Received 08. June 2009 · Accepted 02. December 2009

Summary: In this study, we analyzed the 20th century ice volume changes for 20 glaciers in the south-eastern Swiss Alps. Our sample included different glacier geometries, sizes and exposures and allowed us to investigate glacier response to climate change. Using a distributed accumulation and temperature-index melt model, we derived mass balance time series in seasonal resolution from 1900. The model was calibrated using ice volume changes obtained from differentiating digital elevation models based on (i) terrestrial topographic surveys, (ii) the Shuttle Radar Topographic Mission (SRTM), and (iii) aerial photogrammetry. In-situ point measurements of annual mass balance and winter accumulation were available for some glaciers, and long-term discharge records were used for model validation. The rate of mass loss between 1900 to 2008 strongly differed between adjacent glaciers. Whereas large valley glaciers (e.g. Vadrec del Forno) showed average mass balances of up to -0.60 m w.e. a^{-1}, smaller and steeper glaciers (e.g. Vadret da Palü) exhibited slower mass loss in the order of -0.20 m w.e. a^{-1}. Over the last century, the regional ice volume decreased by 47%, with strong differences between individual glaciers (30–75%). Using a combined model for 3D glacier evolution and stream-flow runoff driven by regional climate scenarios, we generated perspectives for the 21st century. We determined a decrease in glacier area of 63% until 2050 and an increase in annual discharge over the next three decades for catchments with high glacierization. By 2100, the model results indicated a shift in the hydrological regime and a 23% decrease in annual runoff attributed to increased evapotranspiration and strongly reduced glacier melt contribution.

Zusammenfassung: In dieser Studie analysieren wir die Eisvolumenveränderungen im 20. Jahrhundert für 20 Gletscher in den südöstlichen Schweizer Alpen. Unsere Auswahl enthält Gletscher verschiedener Typen, Größen und Expositionen. Dies ermöglicht eine Untersuchung der Reaktion der Gletscher auf die aktuelle Klimaerwärmung. Durch die Anwendung eines verteilten Akkumulations- und Temperatur-Index-Schmelzmodells werden Massenbilanz-Zeitreihen seit 1900 in saisonaler Auflösung berechnet. Die Kalibrierung des Modells erfolgt mittels Eisvolumenveränderungen. Diese wurden durch verschiedene digitale Höhenmodelle, basierend auf (i) topographischen Karten, (ii) der Shuttle Radar Topographic Mission (SRTM), und (iii) Luftbildauswertungen gewonnen. Für die Modell-Validierung kommen sowohl in-situ Punkt-Messungen der jährlichen Massenbilanz und der Winterakkumulation, die für einige Gletscher zur Verfügung stehen, als auch Langzeit-Abflussmessungen zum Einsatz. Die Rate des Massenverlustes zwischen 1900 bis 2008 unterscheidet sich stark zwischen benachbarten Gletschern. Während große Talgletscher (z.B. Vadrec del Forno) eine durchschnittliche Massenbilanz von bis zu -0.60 m w.e. a^{-1} aufweisen, zeigen kleinere und steilere Gletscher (z.B. Vadret da Palü) einen geringeren Massenverlust in der Größenordnung von -0.20 m w.e. a^{-1}. Im Laufe des letzten Jahrhunderts ist das regionale Eisvolumen um 47% zurückgegangen, mit grossen Unterschieden zwischen den einzelnen Gletschern (30–75%). Mittels eines kombinierten 3D-Gletscherentwicklungs- und Abflussmodells, angetrieben durch regionale Klimaszenarien, generieren wir Perspektiven für das 21. Jahrhundert. Die Modellierung prognostiziert einen Rückgang der Gletscherfläche von 63% bis ins Jahr 2050. Während den nächsten drei Jahrzehnten erkennen wir einen Anstieg des jährlichen Abflusses für stark vergletscherte Einzugsgebiete. Bis 2100 zeigen die Resultate eine Verschiebung des hydrologischen Regimes und einen Rückgang des Jahresabflusses von 23%. Dieser ist auf eine erhöhte Evapotranspiration und einen stark reduzierten Beitrag der schmelzenden Gletscher zurückzuführen.

Keywords: Glacier retreat, ice volume change, mass balance modelling, glacier runoff, Vadret da Morteratsch

1 Introduction

Since the 1850s, the end of the Little Ice Age, glaciers in the European Alps have suffered major ice volume losses (Vincent 2002; Kaser et al. 2006; Steiner et al. 2008). The effect of changes in climate forcing on glaciers is most clearly reflected in their surface mass budget. Long-term glacier mass balance observations are indispensable to investigate how climate acts on glaciers (Vincent et al. 2004;

DOI: 10.3112/erdkunde.2010.02.02 ISSN 0014-0015 http://www.erdkunde.uni-bonn.de

Ohmura et al. 2007). However, mass balance time series in the Alps are typically short and only cover a few relatively small glaciers, leaving entire glacierized regions unobserved (Zemp et al. 2009). Furthermore, the difference in the rate of mass loss of individual glaciers is large (e.g. Kuhn et al. 1985; Huss et al. 2008a; Paul and Haeberli 2008), resulting in a high uncertainty in extrapolating glacier mass balance to unmeasured glaciers. In the near future, a substantial retreat of Alpine glaciers is expected (e.g. Maisch 2000; Zemp et al. 2006; Jouvet et al. 2009), leading to major impacts on water resource management (Zierl and Bugmann 2005; Horton et al. 2006; Stahl et al. 2008), tourism (Bürki et al. 2003) and natural hazards (Richardson and Reynolds 2000). Providing realistic scenarios for future impacts of climate warming on the environment is highly important for alpine communities in order to adapt to the rapid changes currently occurring.

The south-eastern Swiss Alps have a substantial glacier cover that clusters around the 4000 m high summit of Piz Bernina. In total, there are about two dozen individual glaciers in the region, several of them prominent valley glaciers. So far, glaciological research has mainly addressed Vadret da Morteratsch. The local surface energy balance (Oerlemans 2000; Oerlemans and Klok 2002; Oerlemans et al. 2009), the glacier mass budget (Klok and Oerlemans 2002; Klok and Oerlemans 2004; Machguth et al. 2008; Nemec et al. 2009) and glacier dynamics (Oerlemans 2007) were investigated. Hoelzle and Haeberli (1995) estimated the ice volume and the mean mass balance for several glaciers in the study region based on glacier inventory data and observed length change between 1850 and 1973.

In this study, we analyzed the temporal and spatial changes in 20 glaciers in south-eastern Switzerland between 1900 and 2008. The glaciers investigated represent all of the ice masses in the region and cover different glacier geometries, sizes and exposures. We compiled a comprehensive field data basis incorporating all available measurements from the 20th century originating from various sources: repeated topographical information, long-term runoff records, in-situ seasonal mass balance measurements and observations of glacier length change. These data were used to constrain a distributed glacier mass balance model (Hock 1999; Huss et al. 2008a) driven by daily meteorological variables. Seasonal glacier mass balance time series since 1900 that allow us to study the response of a 20-glacier sample to current climate warming are presented. A glacio-hydrological model (Huss et al. 2008b) is run into the future based on regional climate scenarios, providing estimates of the impact of climate change on glacier extent and the hydrological cycle in the south-eastern Swiss Alps.

2 Study sites and field data

2.1 Study sites

The 20 investigated glaciers, which are located in the south-eastern Swiss Alps, are representative for all of the significant ice masses in this mountain range (Fig. 1). The glaciers are located in the head watersheds of three valleys, which drain to the north-east (Engadine), to the south (Val Poschiavo) and to the south-west (Val Bregaglia). The size of the studied glaciers ranges from 0.3 km² to 16 km² and they occupied a total area of 62 km² in 2003. Theses glaciers represent a wide range of different glacier types (Fig. 1 and Tab. 1). The long-term equilibrium line altitude (ELA) is at around 3000 m a.s.l. for the eastern glaciers of the study area and drops to 2600 m a.s.l. towards the west, indicating a regional precipitation gradient. The study area contains two typical valley glaciers (Vadret da Morteratsch, Vadrec del Forno) and several other prominent ice masses (e.g. Vadret da Palü, Vadret da Roseg, Vadret da Tschierva) (Fig. 1). The glaciers in the Val Bregaglia are often situated in cirques and are fed by avalanches and wind-deposited snow. The tongue of Vadrec da l'Albigna is debris-covered. Its retreat rate accelerated after the late 1950s due to a proglacial reservoir.

2.2 Digital elevation models and ice volume changes

As the most important and new data source we compiled a set of three to six high-resolution digital elevation models (DEMs) and glacier outlines covering the entire 20th century for each of the investigated glaciers. The topographical information originated from various sources; hence, different techniques are applied to generate the DEMs. In general, we obtained (i) DEMs for the 1930s and the 1950s from digitizing topographic maps, (ii) a DEM for 1991 from the digital terrain model of the Swiss topographic survey (DHM25 level1), (iii) a coarse resolution DEM for February 2000 based on the Shuttle Radar Topographic Mission (SRTM), and (iv) high-accuracy DEMs of the years 1985 and 2008 for selected glaciers (Tab. 1) produced by photogram-

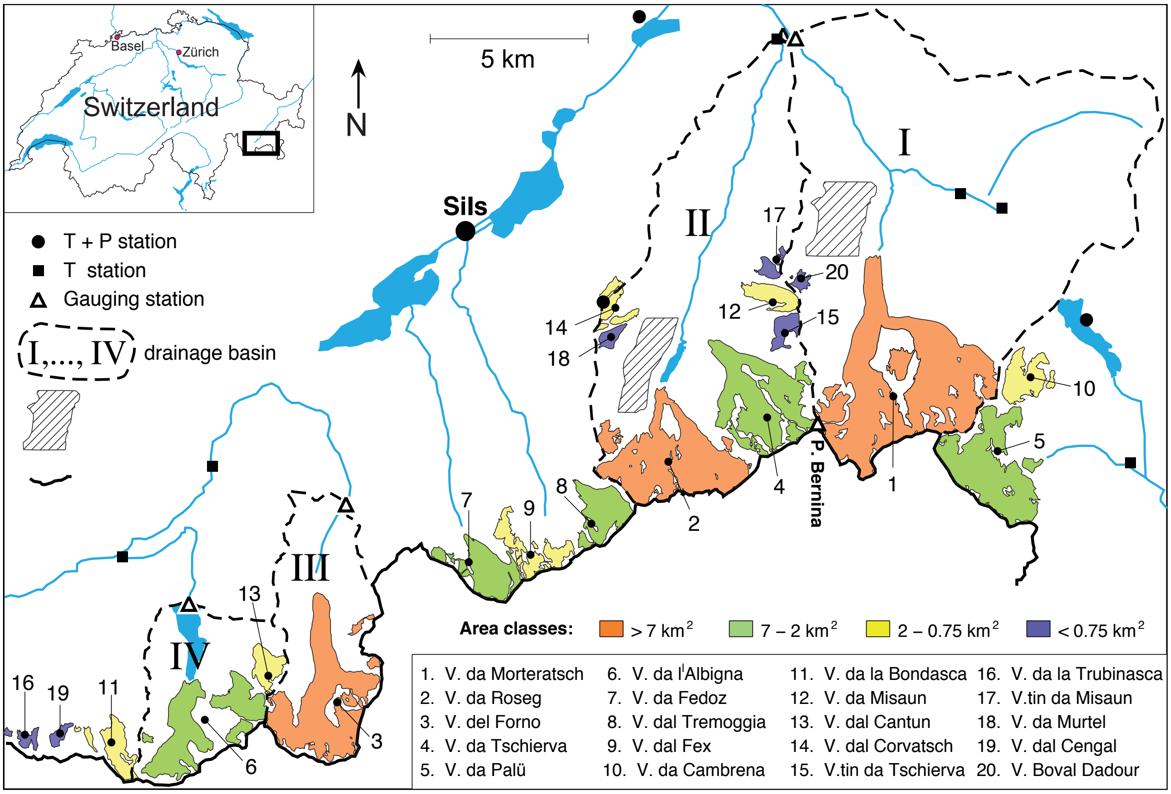

Fig. 1: Overview map of the study area. All investigated glaciers are shown with their extent in 2003. The colour of the glaciers visualizes their size. Relevant weather stations are indicated with symbols (T: temperature, P: precipitation). Investigated drainage basins I-IV are shown with dashed lines (see Tab. 2 for more information). The glacier-free areas near Vadret da Morteratsch and Roseg used for uncertainty analysis of the digital elevation models are hatched

metric evaluation of aerial photographs. The repeated DEMs are then used for the calculation of distributed ice thickness changes (Fig. 2a) and ice volume changes in periods of one to three decades (Bauder et al. 2007). To convert ice volume to mass change, we assume a density of $\varrho_{\Delta V}$=850 kg m^{-3} (Sapiano et al. 1998).

The topographic map of the years 1934–1942 (date depending on glacier, see Tab. 1) is based on terrestrial topographic surveys and the map of 1955/56 refers to the first evaluation of aerial photographs by the Swiss Federal Office of Topography (SwissTopo). The maps have a scale of 1:50 000 and 1:25 000, respectively. Glacier outlines and elevation contours were digitized in the georeferenced image and interpolated to a regular 25 m grid. We additionally digitized the first topographic map acquired in about 1850. However, its elevation accuracy was judged to be insufficient for the calculation of an ice volume change and we only used the glacier outlines for visualization purposes (Fig. 2)

The comparison of the SwissTopo DHM25 level1 product and the SRTM elevation model was proposed by Paul and Haeberli (2008) for calculation of ice thickness changes over a 15-year time period. As both datasets are easily available and cover the entire Swiss Alps, the method has substantial potential. However, several inconsistencies complicate the calculation of ice volume changes. These problems need to be accounted for and the resulting uncertainties critically addressed. First, the exact dating of the DHM25 level1 product is difficult. Whereas it originated from the year 1985 according to SwissTopo and Paul and Haeberli (2008), we found evidence that this is not the case in the south-eastern Swiss Alps. Comparison of DHM25 level1 to DEMs based on aerial photographs taken on August 21, 1985 consistently shows systematic differences. We thus conclude that in the study region, the DHM25 product is based on the subsequent topographic survey of SwissTopo from the year 1991. Second, the estimated overall accuracy of the SRTM data is ±30 m (Jarvis et al. 2008), which would make a reliable calculation of glacier elevation changes impossible. Paul and Haeberli (2008) detected a significantly better performance for Switzerland and assumed the error to

Tab. 1: Compilation of all investigated glaciers and field data basis. Glacier area, ice volume and elevation range refer to the year 1991. Periods covered with discharge measurements and in-situ mass balance observations are given for each glacier individually. The number and the dates of digital elevation models (DEMs) are indicated

Glacier	Area (km^2)	Volume (km^3)	Elevation (m a.s.l.)	Discharge	Mass balance annual	Mass balance winter	Number of DEMs
Vadret da Morteratsch	16.58	1.240	2057–4005	1955–2008	1949–59; 91–2007	1949–1959	6 (1935,1955,1985,1991,2000,2008)
Vadret da Roseg	8.79	0.350	2214–3599	1955–2008			6 (1935,1955,1985,1991,2000,2008)
Vadrec del Forno	7.96	0.660	2265–3365		1955–1960	1955–1960	4 (1937,1956,1991,2000)
Vadret da Tschierva	6.37	0.240	2202–3980	1955–2008			6 (1935,1955,1985,1991,2000,2008)
Vadret da Palü	6.24	0.270	2326–3822				5 (1934,1964,1985,1991,2000)
Vadrec da l'Albigna	5.21	0.260	2186–3288	32–55; 94–06	1955–1960	1955–1960	4 (1942,1956,1991,2000)
Vadret da Fedoz	2.63	0.120	2542–3341				4 (1935,1955,1991)
Vadrec dal Tremoggia	2.23	0.100	2637–3284				4 (1935,1955,1991)
Vadret da Fex	1.83	0.067	2497–3341				3 (1935,1955,1991)
Vadret dal Cambrena	1.83	0.077	2517–3414				5 (1934,1964,1985,1991,2008)
Vadrec da la Bondasca	1.51	0.071	2024–3263				3 (1942,1956,1991)
Vadret da Misaun	0.96	0.041	2737–3498	1955–2008			3 (1936,1955,1991)
Vadrec dal Cantun	0.93	0.033	2598–3284	32–55; 94–06	1955–1960	1955–1960	3 (1942,1956,1991)
Vadret dal Corvatsch	0.88	0.030	2817–3422	1955–2008			3 (1935,1955,1991)
Vadrettin da Tschierva	0.74	0.025	2956–3607	1955–2008			3 (1935,1955,1991)
Vadrec da la Trubinasca	0.46	0.011	2175–2794	1955-2008			5 (1942,1955,1985,1991,2008)
Vadrettin da Misaun	0.44	0.012	2846–3228	1955–2008			5 (1936,1956,1985,1991,2008)
Vadret da Murtel	0.41	0.012	3010–3374				3 (1935,1955,1991)
Vadrec dal Cengal	0.34	0.009	2006–2563				3 (1942,1956,1991)
Vadret Boval Dadour	0.30	0.007	2836–3184	1955–2008			3 (1935,1955,1991)

be randomly distributed. Paul (2008) also reported evidence against the previously suspected elevation bias in SRTM data (e.g. Berthier et al. 2006). We downloaded the SRTM data set version 4 from http://srtm.csi.cgiar.org (Jarvis et al. 2008).

A drawback of the SRTM data set is its coarse resolution of about 90 m, which is insufficient for resolving small scale features in alpine terrain. Especially in rugged topography of cirques surrounded by steep walls, occupied by small glaciers, the resolution-induced uncertainty is considerable. Thus, we did not use the SRTM DEM for glaciers with areas of less than 3 km². For the calculation of 1991–2000 elevation changes, we interpolated both the DHM25 and SRTM elevation model to a regular 100 m grid. In order to compute the change in ice volume, glacier outlines must be known. They were digitized from the 1:25 000 topographic map for 1991. For obtaining up-to-date information on glacier extent, we used a comprehensive data set of orthorectified aerial photographs (SwissImage) with a spatial resolution of 0.5 m provided by SwissTopo. The photographs available for the study site were acquired in the summer of 2003 and allowed accurate tracking of the glacier extent due to good contrast because of the almost complete melt-out of the glaciers. The outlines for 2003 were digitized for all investigated glaciers and provided ice extent based on a consistent data basis (Fig. 1).

The SRTM DEM was acquired in February 2000. Thus, the effect of the snow cover evolution since fall 1999 needed to be corrected when calculating changes in ice volume. We accounted for this factor by estimating the snow depth accumulated on the glaciers between October 1999 and February 2000 using meteorological data and assuming a snow density of $\varrho_{Feb} = 300\,kg\,m^{-3}$. This resulted in a snow depth of 2-3 metres.

Aerial photographs for August 1985 and September 2008 were available for Vadret da Morteratsch, Roseg, Tschierva and some smaller glaciers (Tab. 1), thus covering more than half of the glacierized area in the study region. They were evaluated using digital photogrammetry and high-accuracy DEMs were produced. We performed an intercomparison of all DEMs and an integrative uncertainty analysis in two ice-free areas near Vadret da Morteratsch and Roseg (Fig. 1, see 'Uncertainty analysis').

2.3 Discharge and mass balance data

For several decades, discharge from the major catchments in the study area has been gauged (Fig. 1) resulting in long-term discharge records. Daily data for the catchments of Morteratsch and Roseg/ Tschierva have been provided by the Federal Office for the Environment (BAFU) since 1955. Discharge records from the Albigna catchment available in daily resolution for 1932 to 1955, and in monthly resolution for 1994 to 2006. Data are provided by Elektrizitätswerke Zürich (EWZ). We also focused on the Vadrec del Forno catchment upvalley of a water intake of EWZ. The current glacierization of the drainage basins is between 15% and 35% (Tab. 2). The two eastern catchments (I,II) exhibit significantly lower mean annual runoff, attributed to less precipitation and higher evapotranspiration losses.

For the investigated glaciers, there are no long-term records aiming at the determination of the glacier-wide mass balance available. However, several measurements series at single locations can be found in the literature and were used in this study. In the 1950s, G. Gensler observed seasonal to annual accumulation rates on top of several hanging glaciers in the Morteratsch region by binocular (FIRNBERICHTE 1914–1978). On both Vadrec del Forno and Vadrec da l'Albigna, mass balance measurements at a network of 11 stakes (Fig. 2b) were performed between 1955 and 1960 (VAW 1962). Additionally, observations of the winter accumulation are available for most of the stake locations on these glaciers. For four sites in the ablation area of Vadret da Morteratsch (Fig. 2a), mass balance records for the last decade were performed by Utrecht University (OERLEMANS 2000; MACHGUTH et al. 2008; OERLEMANS et al. 2009). PALMER et al. (2003) report on an ice core at a high accumulation site below Piz Zupo (Vadret da Morteratsch) at almost 3900 m a.s.l. Between 1991 and 2001, annual accumulation rates of between 2.4 and 4.3 m w.e. were determined. The accumulation mainly occurred during summer snowfall events (PALMER et al. 2003).

Continuous annual observations of retreat or advance of the glacier terminus since the late 19th century are available for the glaciers Morteratsch, Roseg, Forno, Tschierva, Palü and Cambrena (GLACIOLOGICAL REPORTS 1881–2009). The interpretation of length change data in climate impact studies is complicated by glacier response time and is thus not straightforward (HOELZLE et al. 2003; OERLEMANS 2007). Here, we use glacier length data as an independent source for comparison with our mass balance results.

3 Methods

In order to homogenize, unify and interpret the discontinuous field data, which originated from various sources, we used modelling driven by meteorological data in daily resolution. This allowed us to derive continuous and comparable mass balance time series for all glaciers over the 20th century. The glacier mass balance model (HUSS et al. 2008a) was used as a tool for the temporal and spatial downscaling of the field data, as it is directly constrained by them. All components of our methodology are briefly described hereafter.

3.1 Meteorological time series

For generating continuous and consistent meteorological time series scaled to each study site for 1900 to 2008, we relied on a combination of different data types. For all study sites, daily air temperature fluctuations from the MeteoSwiss station at Sils (Fig. 1) were used. Additionally, homogenized monthly means (Fig. 3a) that were available for Sils (BEGERT et al. 2005) were used to correct the daily series. Temperature gradients with elevation were determined for each glacier individually based on a comparison of several nearby weather stations with

Tab. 2: Investigated drainage basins. The glacierization of the catchments is provided for 1955 and 2003. $\overline{\varrho_{1961\text{-}90}}$ is the measured (catchments I,II) and simulated (III,IV) mean specific discharge over the climatic normal period 1961-1990

ID	Catchment	Area (km^2)	$Glac_{1955}$ (%)	$Glac_{2003}$ (%)	$\overline{\varrho_{1961\text{-}90}}$ (mm)
I	Morteratsch	108.1	17.5	15.2	1301
II	Roseg	67.2	28.2	25.8	1269
III	Forno	22.2	43.3	34.4	3093
IV	Albigna	19.0	38.0	30.3	2809

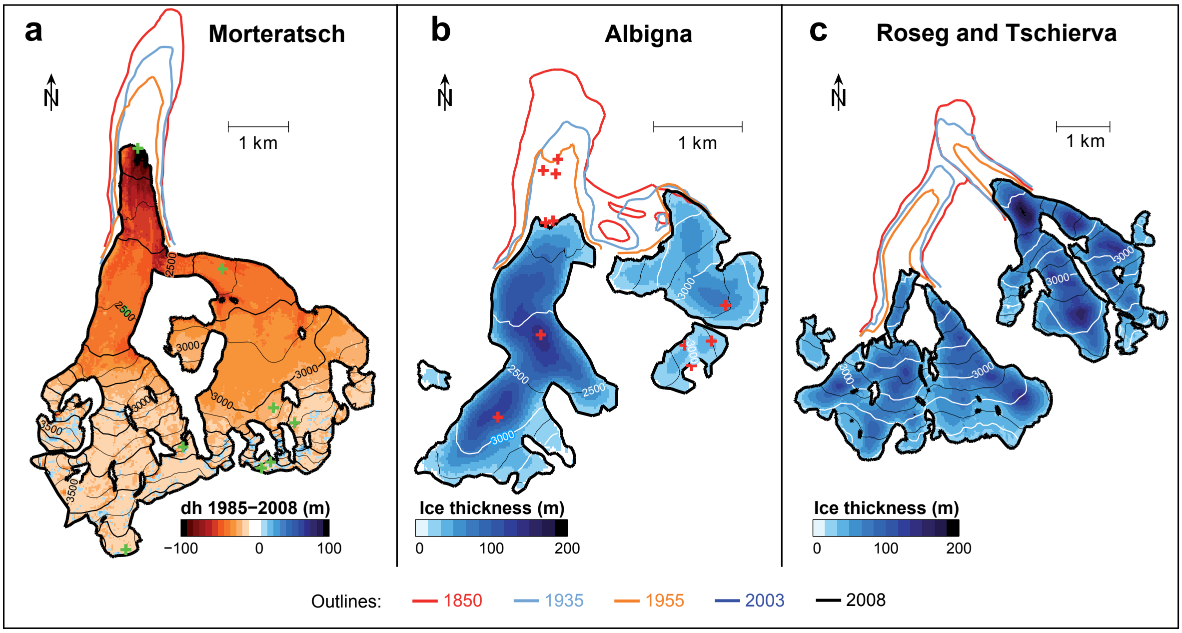

Fig. 2: Topographical setting and selected field data basis for three important glaciers. Observed glacier outlines over the last 150 years are shown for all glaciers documenting their significant retreat. (a) Vadret da Morteratsch. The colours indicate the distribution of surface elevation changes between 1985 and 2008 based on comparison of two DEMs. The location of mass balance stakes (GLACIOLOGICAL REPORTS 1881-2009; OERLEMANS 2000; PALMER et al. 2003) used for model calibration is indicated by crosses. (b) Vadrec da l'Albigna. The inferred ice thickness distribution is shown. The network of mass balance stakes surveyed in the year 1955 is displayed. (c) Ice thickness distribution of Vadret da Roseg and Vadret da Tschierva. Note that the scales differ between the subfigures. The interval of glacier surface contour lines is 100 m

shorter time series (Fig. 1). The regional distribution of precipitation and the monthly sums in 1971–1990 are provided by a gridded precipitation map for the Alps (PRISM) with a resolution of 2 km (SCHWARB et al. 2001). For each glacier, one weather station with long precipitation series well representing the immediate vicinity of the glacier was selected (Fig. 1). The measured daily precipitation was scaled to the grid cell of the PRISM data set over the glacier and provided the temporal precipitation fluctuations (Fig. 3b).

3.2 Mass balance model description

We applied a distributed accumulation and temperature-index melt model to calculate the glacier surface mass balance components (HOCK 1999; HUSS et al. 2008a). Degree-day factors were varied as a function of potential direct radiation in order to account for the effects of slope, aspect and shading. Daily surface melt rates $M=M(x,y,t)$ at day t and for grid cell (x,y) of the digital elevation model were computed by

$$M = \begin{cases} (f_M + r_{snow/ice} I_{pot})T & : \quad T > 0°C \\ 0 & : \quad T \leq 0°C \end{cases} \qquad (1)$$

where f_M denotes a melt factor, $r_{snow/ice}$ are radiation factors for ice and snow surfaces (see table 3 for units) and $I_{pot} = I_{pot}(x,y,t)$ is the potential solar radiation. Air temperature $T = T(x,y,t)$ is determined using a constant lapse rate dT/dz and the elevation of the weather station z_{WS}:

$$T(x,y,t) = T_{WS}(t) + (z(x,y) - z_{WS}) \cdot dT/dz \qquad (2)$$

Below 3500 m a.s.l., precipitation was assumed to increase linearly with elevation (dP/dz). A correction factor c_{prec} allowed the adjustment of precipitation sums and a threshold temperature T_{thr}=1.5 °C distinguished snow from rainfall (HOCK 1999). The spatial variation in accumulation over the glacier surface was substantially influenced by the preferential deposition of snow and snow redistribution (LEHNING et al. 2008). These effects were taken into account by using a spatial snow distribution multiplier $D_{snow}(x,y)$ derived from terrain characteristics (HUSS et al. 2008a). Snow accumulation $C=C(x,y,t)$ was calculated based on the measured precipitation at the weather station $P_{WS}(t)$ occurring at temperatures $T(x,y,t) < T_{thr}$ as

$$C = P_{WS}(t) \cdot c_{prec} [1 + (z(x,y) - z_{WS}) \cdot dP/dz] \cdot D_{snow}(x,y) \qquad (3)$$

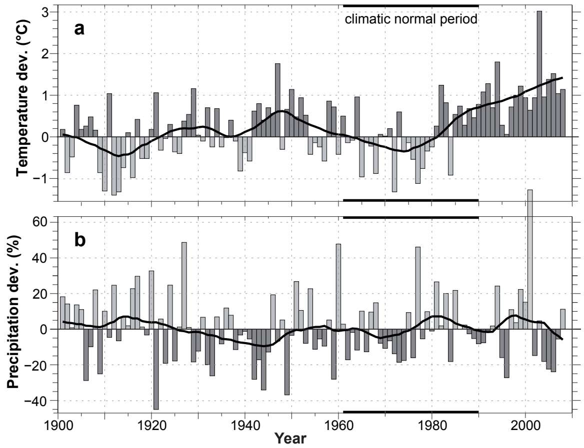

Fig. 3: Homogenized meteorological time series of MeteoSwiss (Begert et al. 2005) for Sils: Deviations from the 1961-1990 climatic normal period of (a) summer temperature (May to September) and (b) annual precipitation are shown. Solid lines indicate 11-year running means

3.3 Determination of ice thickness distribution

Ice volume and ice thickness distribution are the basic initial conditions for impact studies addressing future glacier retreat. They exert an important control on the hydrological response to climate change, and on ice flow dynamics. Several methods have been developed to estimate the ice volume of alpine glaciers from readily available field data such as glacier area and mean glacier slope (e.g. Haeberli and Hoelzle 1995; Bahr et al. 1997). Farinotti et al. (2009a) have proposed a new approach for calculating distributed ice thickness, and consequently the bedrock elevation, based on glacier surface topography only. The developed Ice Thickness Estimation Method (ITEM) was applied to infer the total ice volume in the Swiss Alps (Farinotti et al. 2009b) and is used to obtain ice volume estimates and bedrock topographies for all investigated glaciers in this study.

ITEM requires a DEM of the glacier surface, glacier outlines, and longitudinal flowlines as input. Ice volume fluxes for every point along the flowline are calculated based on altitudinal mass balance gradients corrected with the long-term surface elevation change (Farinotti et al. 2009b). Using an inverted form of Glen's flow law (Paterson 1994), ice thickness was derived and interpolated spatially by taking into account information contained in the local surface slope of every grid cell. A tuning factor in the ice flow law, accounting for valley shape and sliding, was calibrated for 13 Swiss glaciers with direct ice thickness measurements (Farinotti et al. 2009a).

Examples for the inferred ice thickness distribution are shown in figures 2b and c. We find maximum ice thicknesses of 300 m for Vadret da Morteratsch and 200 m for Vadrec del Forno. For the steeper Vadret da Roseg, ice thicknesses only reach 130 m and smaller glaciers often exhibit maximum thicknesses of less than 60 m (e.g. Vadrec da la Bondasca).

3.4 Glacier Evolution Runoff Model (GERM)

For the calculation of runoff from the drainage basins with discharge records (Fig. 1 and Tab. 2), we applied the glacio-hydrological model GERM (Glacier Evolution Runoff Model), which is described in detail in Huss et al. (2008b). This model relies on the glacier mass balance computations outlined above and additionally includes modules for the change in 3D glacier geometry with climate warming, evapotranspiration and runoff routing. In this study, we used GERM in a first step to calculate runoff over the past five decades, which can then be compared to observations, and, in a second step, to generate future perspectives for glacier evolution and changes in the hydrological regime over the 21st century.

A central element in GERM that distinguishes it from other hydrological models applied in the European Alps (e.g. Braun et al. 1994; Horton et al. 2006; Schaefli et al. 2007) is that the change in ice volume and glacier extent is modelled transiently. This allows the analysis of runoff changes in highly glacierized drainage basins. The module to update glacier surface requires a DEM of the glacier surface and the bedrock topography generated using ITEM as input. The annual change in ice volume calculated using the mass balance model is converted into a distributed ice thickness change applying a so called Δh-parameterization (Huss et al. 2010). The Δh-parameterization prescribes the change in glacier surface elevation along the glacier in response to a given surface mass balance. It is based on the observation that elevation changes of retreating glaciers are normally largest near the glacier terminus (see Fig. 2a) and smaller in the accumulation area (e.g. Arendt et al. 2002; Bauder et al. 2007), which is confirmed also in theory (Jóhannesson et al. 1989). Δh-parameterizations are derived for each glacier individually from the observed distributed ice thickness change between the first and the last DEM available (Tab. 1). Comparison of glacier geometry change over the 21st century, simulated using the Δh-parameterization and 3D ice flow modelling (Jouvet et al. 2009), has shown good agreement (Huss et al. 2010) indicating that our simplification of ice flow dynamics is a reasonable and a computationally cheap approach for modelling future glacier evolution. The method is mass conserving and applicable to any glacier without any other field data requirements than readily available land surface DEMs.

In GERM, evaporative losses are calculated using an empirical approach (Hamon 1961) based on air temperature and potential solar radiation. The evapotranspiration model distinguishes five surface types (ice, snow, rock, low vegetation, forest), has an interception reservoir and calculates the actual evaporation based on the saturation of the soil reservoir (Huss et al. 2008b). For model runs over the 21st century the expected increase in the tree-line altitude and the rise of the upper boundary of vegetation (Burga 1999; Theurillat and Guisan 2001) are accounted for in 20-year intervals. Runoff is routed through the system using six dynamically changing linear reservoirs referring to the five surface types and a slow ground water system (Huss et al. 2008b).

3.5 Model calibration

The mass balance model is calibrated for each glacier individually. The melt parameters f_M and $r_{ice/snow}$ (see Eq. 1) are varied such that in each subperiod between two successive DEMs the observed ice volume change is matched by the modelled one. The rate of the decadal glacier mass change is thus given by DEM differencing; the temporal variability is obtained from the daily meteorological data. The melt parameters are allowed to vary between the DEM subperiods in order to exactly reproduce the observed volume change. We detected variations in the parameter values of ±10% with a general decrease over the last decades for all glaciers. This long-term reduction in the degree-day factors of empirical temperature-index modelling is explained by their oversensitivity to temperature changes (Pellicciotti et al. 2005; Huss et al. 2009b). Additional field data – discharge measurements and mass balance observations (Tab. 1) – allow iterative adjustment of the parameters steering the distribution and the amount of accumulation (dP/dz, c_{prec}, see Eq. 3). The accumulation parameters, regarded as external meteorological boundary conditions were kept constant over the entire modelling period. The calibrated model reasonably reproduced the observed annual runoff volumes (mean deviation <1%), and the hydrological regime in all drainage basins with discharge measurements (Fig. 4). We obtained a Nash and Sutcliffe (1970)-criterion of $R^2=0.88$ for monthly runoff.

By combining all available field data and using them to constrain the mass balance model, we obtained an optimal set of melt and accumulation parameters for each glacier (Tab. 3). Our mass balance results in high temporal and spatial resolution thus correspond to the observed changes in ice volume, reproduce the observed altitudinal mass balance gradients and provide a closure of the water balance in the drainage basins. Hence, we use several types of discontinuous and per se incomplete field data sets, merged with meteorological information, for producing consistent long-term glacier mass balance series.

For glaciers with only ice volume changes available for calibration, the accumulation parameters were set to values that were obtained for neighbouring glaciers. The DEMs do not span the entire period of interest; for the years before the first DEM (1900–1930s), we used the parameter set calibrated for the first DEM subperiod and parameters calibrated for the last DEM subperiod are used after the latest DEM (Tab. 1).

3.6 Uncertainty analysis

We performed two types of integrative uncertainty analysis aiming at quantifying the accuracy and possible biases in each DEM used to derive ice volume changes. (1) We compared all DEMs in two glacier-free test areas near Vadret da Morteratsch and Roseg (Fig. 1). (2) We investigated the suitability of the SRTM DEM – the data source with the highest nominal error in the elevation information – for calculating glacier mass balance time series. We also discuss the effect of uncertainties in the DEMs on the final mass balance time series.

The two test areas (2.7 km² and 2.9 km²) range from 2200 to 2900 m a.s.l. (Fig. 1). Both are covered by all DEMs available except for the Morteratsch test site in the years 1985 and 2008. In these years the comparison was only performed for the Roseg test site. We compared all data sources to each other on a 25 m grid and evaluated the mean elevation difference (expected to equal zero) and the standard deviation (Tab. 4). The SRTM DEM was corrected for the snowcover in February 2000. For comparison of SRTM with other DEMs, these were resampled as proposed by Paul (2008) in order to eliminate resolution dependent effects.

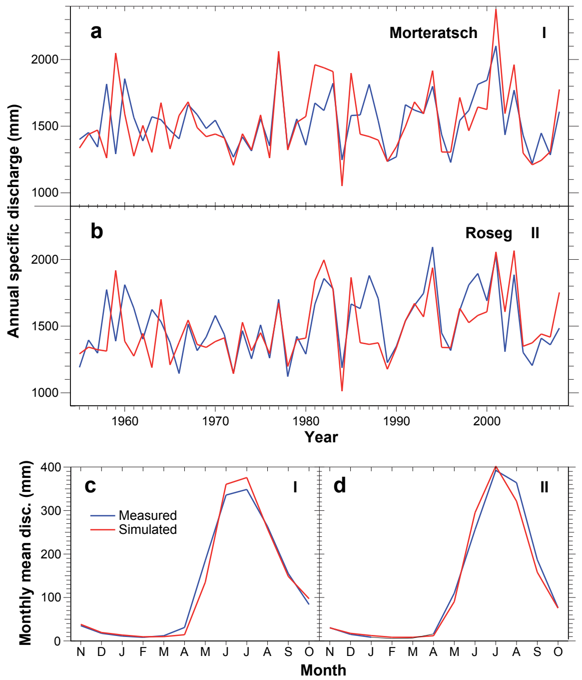

Fig. 4: (a, b) Comparison of simulated against observed specific annual runoff volume (discharge divided by catchment area) for drainage basins I and II. (c,d) Simulated and observed mean specific monthly runoff regime over the period 1955–2008 for basins I and II

In the glacier-free test areas, most DEMs except the SRTM DEM, yield the same average elevation within ±2 m (Tab. 4). The best agreement (Δ=0.05 m) is found for the comparison of the two DEMs based on photogrammetry (1985, 2008) assumed to have to highest accuracy. Standard deviations of the elevation difference between two DEMs are typically around 5 m. The SRTM DEM, however, exhibits a significant bias compared to all other independently derived DEMs of 6–7 m, except for 1934 (Tab. 4). This offset indicates a systematically too high surface topography in the glacier-free area. Berthier et al. (2006) report an elevation gradient in the SRTM bias in the western Alps, with an overestimation of the actual surface elevation below about 2500 m a.s.l. and underestimation above. For the calculation of long-term elevation and ice volume changes DEMs that agree in glacier-free areas are crucial. Our DEM intercomparison shows that the DEMs established based on topographic maps are roughly consistent with the DHM25 level1 and high-accuracy photogrammetry and can thus be used to determine geodetic mass balances.

In addition to the DEM intercomparison in the glacier-free test site, we also evaluated disagreement of the SRTM DEM and digital photogrammetry on a glacier-wide scale, and thus investigated the suitability of the SRTM DEM to derive ice volume changes. We performed two calibration-validation experiments for Vadret da Morteratsch, Roseg and Tschierva. First, we calibrated the mass balance model on the ice volume change 1985–2008, which is based on two photogrammetric surveys and is thus highly accurate (see also Tab. 4). We evaluated the disagreement of the calculated cumulative annual volume change in 2000 with the SRTM derived ice volume change 1985–2000 (red dots in Fig. 5). The misfit between the calculated mass balance curve and the geodetic volume change in 2000 is substantial and underlines the finding of the DEM intercomparison: Differencing of the 1985 DEM and SRTM yields too small mass loss, comparison of SRTM with the 2008 DEM implies too fast mass loss (Fig. 5). The misfit in ice volume in 2000 can be explained with a bias of 6–7 m in the SRTM DEM, which corresponds to the misfit assessed in the glacier-free area (Tab. 4).

In a second experiment, we calibrate the mass balance model using the observed ice volume change 1985–2000 and then forecast mass balance for the period 2000–2008. The misfit of the calculated ice volume change in 2008 with the observed one is considerable (blue asterisks in Fig. 5). Cumulative mass loss over the last two decades would be underestimated by almost 50% when assessing it using the uncorrected SRTM DEM.

Our results show that correcting the SRTM derived DEM is required in order to obtain reasonable geodetic ice volume changes. We assume that the bias of 6 m applies to all glaciers in the study area for which the SRTM is used and introduce a correction of the elevation information. Due to the considerable uncertainty in the SRTM derived volume change we only use this data source for model calibration, when no photogrammetry for 2008 is available and glacier area is larger than 3 km² (3 glaciers). For glaciers where a photogrammetry based DEM for 1985 is available, we also did not use the DHM25 level 1 terrain model for calibration (Tab. 1).

We estimated the accuracy of the calculated mass balance time series based on the uncertainty in the geodetic mass change σ_{geod} constraining the inferred long-term trend in mass loss. In a subperiod between two successive DEMs, is calculated as

$$\sigma_{geod} = \sqrt{\Delta z^2 \cdot \sigma_{\rho}^2 + \rho_{\Delta V}^2 \cdot \sigma_{z}^2} \qquad (4)$$

where $\rho_{\Delta V}$ is the density used to convert ice volume to mass change and σ_{ρ}=50 kg m^{-3} is the assumed

Tab. 3: Calibrated parameters of the mass balance model and units (see Eqs. 1, 2 and 3). The average and the standard deviation σ_{param} of the parameters over all glaciers and time periods is given

Parameter	Units	20-gl. mean	σ_{param}
f_M	10^{-3} m d^{-1} °C^{-1}	0.808	0.136
r_{ice}	10^{-5} m^{3}W^{-1} d^{-1} °C^{-1}	1.940	0.327
r_{snow}	10^{-5} m^{3}W^{-1} d^{-1} °C^{-1}	1.246	0.213
dT/dz	°Cm^{-1}	-0.00521	0.00025
dP/dz	% m^{-1}	0.0385	0.0250
c_{prec}	–	1.463	0.473

uncertainty. Δz is the geodetic elevation change and σ_z is the related uncertainty given by

$$\sigma_z = \sqrt{\sigma_{DEM_1}{}^2 + \sigma_{DEM_2}{}^2} \quad (5)$$

The uncertainty in the DEMs σ_{DEM} depends on (i) the geolocation and orientation of the aerial photographs or maps, (ii) the accuracy of the elevation information and (iii) the interpolation to unmeasured grid points (Thibert et al. 2008; Huss et al. 2009a). Based on the DEM intercomparison (Tab. 4) we assume $\sigma_{DEM,1,2}=\pm 2$ m (1930s, 1950s), $\sigma_{DEM,3}=\pm 1$ m (1991), $\sigma_{DEM,4}=\pm 6$ m (2000) and $\sigma_{DEM,5}=\pm 0.5$ m (1985, 2008). We take into account higher uncertainties in the mass balance time series for the period between 1900 and the first DEM and after the last DEM and find an uncertainty in the rate of the 1900–2008 mass loss of 0.08 m w.e. a^{-1}.

4 Results and discussion

4.1 Glacier mass balance in the 20th century

We present mass balance time series in seasonal resolution for all investigated glaciers over the period 1900 to 2008. Annual mass balance is calculated for the hydrological year (Oct. 1–Sept. 30). The winter balance refers to the period Oct. 1 to April 30 and the summer balance is determined for May 1–Sept. 30. We evaluate 'conventional' specific mass balances in meter water equivalent (w.e.), defined as the mass change over one year divided by that year's glacier surface area (Harrison et al. 2005). Glacier surface elevation and area is updated annually based on linear interpolation between successive DEMs (Huss et al. 2008a).

Our method provides spatially distributed mass balance maps on a 25 m grid for each glacier and every year (Fig. 6). The calculated mass balance reasonably reproduces in-situ point measurements of mass balance (inset in Fig. 6). This highly resolved spatial mass balance distribution provides the required input for 3D ice flow models (e.g. Jouvet et al. 2009), but also allows the direct evaluation of other important variables for impact studies, such as the Equilibrium Line Altitude (ELA), the Accumulation Area Ratio (AAR) and altitudinal mass balance gradients (Fig. 6).

Cumulative mass balance time series of the 20 investigated glaciers over the last century are shown in figure 7. The significant differences in the rate of glacier mass loss are evident. The mean annual balances over the last century differ by a factor of more than four (Tab. 5). Vadrec del Forno shows the most negative cumulative mass balance since 1900 (-66 m w.e.). Vadret da Morteratsch, the largest glacier in the region, also has strongly negative mass balance (-49 m w.e.), whereas Vadret da Palü yields a cumulative balance of -16 m w.e. over the same period. Some small glaciers only experienced insignificant mass loss (e.g. Vadrec dal Cengal, -10 m w.e.).

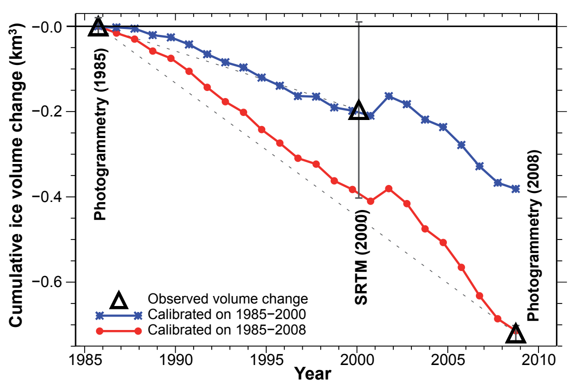

Fig. 5: Validation of the SRTM derived ice volume change using the high-accuracy DEMs of 1985 and 2008, and the mass balance model for Vadret da Morteratsch, Roseg and Tschierva. Results for the three glaciers show coherent trends and were summed up. Triangles indicate the geodetic ice volume change. Error bars are estimated based on the elevation model intercomparison (Tab. 4) and for the DEMs of 1985 and 2008 based integrative error analysis (Huss et al. 2009). Two cumulative series of the calculated annual 3-glacier volume change are shown, (i) calibrated on the observed 1985–2008 volume change (red dots) and (ii) calibrated on the 1985–2000 volume change (blue asterisks)

Tab. 4: Uncertainty analysis in two glacier-free test sites (5.6 km², 9060 grid cells) near Vadret da Morteratsch and Roseg (Fig. 1). All DEMs were compared to one another; the more recent DEM is subtracted from the older one. The difference in elevation averaged over all grid cells is shown below the diagonal (bold), the standard deviation of the elevation difference is given above the diagonal (italic). Note that the SRTM DEM (year 2000) was corrected for the snow cover in mid-February

	1934	1955	1985	1991	2000	2008
			Standard deviation σ(m)			
1934	-	*4.03*	*3.90*	*6.17*	*6.37*	*5.92*
1955	**-1.03**	-	*5.90*	*3.82*	*9.01*	*3.99*
1985	**-1.49**	**-2.00**	-	*3.28*	*9.66*	*1.06*
1991	**-3.74**	**-0.99**	**-0.99**	-	*9.25*	*2.92*
2000	**-4.15**	**-6.99**	**-7.46**	**-6.07**	-	*9.17*
2008	**-2.54**	**0.26**	**-0.05**	**1.26**	**7.39**	-
	mean deviation (m)					

Tab. 5: Changes in individual glaciers over the 20th century and perspectives for the future. The mean rate of mass loss $\overline{b}$ since 1900 and the long-term average equilibrium line altitude $\overline{ELA}$ are given by the mass balance model and field data. The ice volume ratio R_v is defined as the ice volume stored below the median glacier elevation divided by the volume stored above. Ice volume changes ΔV relative to the total ice volume V obtained from ITEM are based on DEM differencing complemented with modelling. Relative changes in glacier area $\frac{\Delta A}{A}$ refer to the period from the mid-1930s to 2003 according to observed glacier outlines (Tab. 1). The estimated area change between 2003 and 2050 and the year of disappearance (glacier area <5% relative to 2003 extent, or <0.1 km²) is calculated using climate scenarios (see Section 'Future perspectives')

ID	Glacier	$\overline{b}_{1900-2008}$ (m w.e. a^{-1})	$\overline{ELA}$ (m a.s.l.)	R_v –	$\frac{\Delta V_{1900-2008}}{V_{1900}}$ (%)	$\frac{\Delta A_{1935-2008}}{A_{1935}}$ (%)	$\frac{\Delta A_{2003-2050}}{A_{2003}}$ (%)	Disapp. (year)
1	Vadret da Morteratsch	-0.45	2989	2.40	-38	-18	-45	2100
2	Vadret da Roseg	-0.50	3044	1.55	-62	-25	-66	2074
3	Vadrec del Forno	-0.61	2796	4.64	-48	-27	-62	2093
4	Vadret da Tschierva	-0.29	2961	1.65	-53	-26	-68	2096
5	Vadret da Palü	-0.15	3105	1.03	-30	-15	-53	2100
6	Vadrec da l'Albigna	-0.49	2748	3.45	-67	-33	-74	2080
7	Vadret da Fedoz	-0.26	2974	1.43	-39	-32	-91	2052
8	Vadret dal Tremoggia	-0.20	3001	1.13	-36	-26	-91	2049
9	Vadret da Fex	-0.30	2940	1.05	-51	-47	-82	2056
10	Vadret dal Cambrena	-0.21	2923	1.35	-45	-31	-70	2063
11	Vadrec da la Bondasca	-0.16	2598	0.96	-29	-36	-40	2100
12	Vadret da Misaun	-0.23	3062	0.96	-44	-25	-88	2052
13	Vadrec dal Cantun	-0.16	2795	1.18	-47	-39	-85	2058
14	Vadret dal Corvatsch	-0.33	3037	0.92	-60	-47	-95	2041
15	Vadrettin da Tschierva	-0.27	3239	0.92	-55	-27	-96	2035
16	Vadrec da la Trubinasca	-0.21	2396	1.12	-51	-57	-45	2095
17	Vadrettin da Misaun	-0.38	3105	1.17	-74	-55	-100	2029
18	Vadret da Murtel	-0.17	3174	1.07	-46	-35	-92	2042
19	Vadrec dal Cengal	-0.09	2249	0.90	-31	-51	-43	2059
20	Vadret Boval Dadour	-0.41	3020	1.23	-74	-62	-78	2040
	20-gl. arithmetic mean	-0.29	2908	1.51	-49	-36	-72	2066
	20-gl. area-weighted mean	-0.39	2946	2.15	-47	-26	-63	2083

In general, large and flat glaciers exhibit faster mass loss than small and steep ice masses (Fig. 7). The arithmetic 20-glacier average mass balance (-0.29 m w.e. a^{-1}) is less negative than the area-weighted average (-0.39 m w.e. a^{-1}), which is dominated by the valley glaciers (Tab. 5). For the set of 20 glaciers we obtained a total ice volume change of -3.5 km³ since 1900.

The current ice volume of the investigated glaciers inferred with ITEM was used to put the calculated 1900–2008 ice volume changes into context. Based on the mass balance time series, we obtain the initial ice volume in 1900 for each glacier individually and calculated the relative volume change over the 20th century (Tab. 5). On average, the investigated glaciers lost almost 50% of their ice volume over the 20th century, ranging from a 75% loss for small glaciers (e.g. Vadrettin da Misaun) to a 30% decrease only for some ice fields (e.g. Vadret da Palü). Surprisingly, the relative change in ice volume is larger for Vadret da Morteratsch (-38%) than for some small, but well-protected glaciers (e.g. Vadrec da la Bondasca) (Tab. 5). The observed area changes are in line with these figures. Whereas small glaciers lost up to half of their area between the mid-1930s and 2003, large glaciers show area changes of 15–20% (Tab. 5), although the terminus position of their tongues has changed dramatically (Fig. 2 and 6).

The highly variable mass balance response of glaciers within a single mountain group to climatic warming is intriguing and indicates that the extrapolation of individual mass balance time series to large glacierized regions (e.g. Raper and Braithwaite 2006; Ipcc 2007) is difficult. Understanding the processes that cause strongly different glacier mass balances under similar variations in climatic forcing is a prerequisite to calculate glacier mass changes for entire mountain ranges, and, thus, to make reliable projections of the contribution of mountain glaciers to future sea level rise. Response times of individual glaciers and their climate sensitivity must be taken into account when analyzing their reaction to climate change (e.g. Chinn 1996). Changes in glacier length illustrate the differing reactions of the glacier termini to climate warming (Fig. 8) being strongly related to the glacier response time. Several studies proposed methods to infer long-term glacier mass balance from length change measurements (e.g. Oerlemans 1994; Hoelzle and Haeberli 1995; Hoelzle et al. 2003). We exploited the length change measurements available for six of the investigated glaciers (Fig. 8) to derive independent five-decadal mass balance estimates that can be compared to our results based on field data and modelling.

We apply a simple scheme based on a continuity formulation (Nye 1960) that considers step changes in climate and a transition of the glacier from one

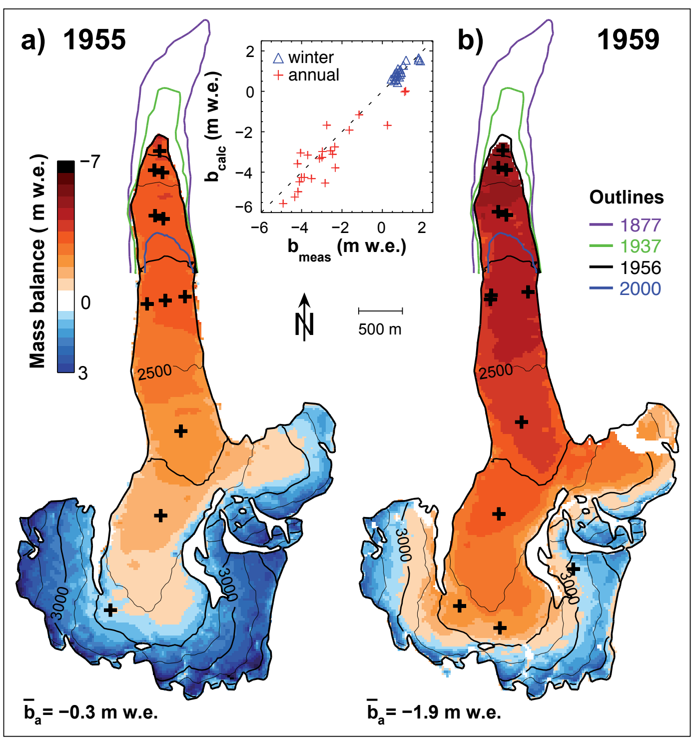

Fig. 6: Spatial distribution of mass balance for Vadrec del Forno in (a) 1955 (balanced mass budget) and (b) 1959 (strong mass loss). The location of in-situ measurements of annual mass balance is indicated with crosses. The comparison of simulated annual and winter balances with direct observations for both years is shown in the inset. Observed glacier outlines throughout the last century are depicted

to another steady-state (Hoelzle et al. 2003). The mean mass balance $\overline{b_{y0-y1}}$ in the period y_0 to y_1 in m w.e. a^{-1} is calculated as

$$\overline{b_{y0-y1}} = \frac{b_t \Delta L \cdot \tau}{2 L_0 (y_1 - y_0)} \quad (6)$$

where b_t is the mass balance at the glacier tongue, ΔL is the observed length change and the initial glacier length (in metres) in year y_0 (Hoelzle et al. 2003). τ is the glacier response time calculated using the approximation of Jóhannesson et al. (1989) as τ=-b_t/h_{max}, with h_{max} the maximal ice thickness in metres. We obtain b_t from the mass balance model and h_{max} from ITEM.

We applied Equation 6 to two 50-year periods in the 20th century for all glaciers with measurements of glacier length (Fig. 8) and compared the length change derived from mean mass balance to model results (Tab. 6). Mass balance obtained from this simple method from length change data corresponds to some degree to the five decadal mass balances given by modelling and ice volume changes, but yield slightly lower rates of mass loss in general (Tab. 6). Discrepancies can be explained by geometrical effects that are neglected in Eq. 6, as well as non-equilibrium conditions. The length change data are useful for roughly estimating the rate of mass loss for different glaciers in low temporal resolution and allow a first distinction of glaciers with high mass loss from glaciers close to equilibrium.

Oerlemans (2007) derived response times of 33 years for Vadret da Morteratsch and only 4 years for Vadret da Palü, both descending from the same mountain (Fig. 1). This result is based on 'backward modelling' using the length record and the assumption that the changes in ELA over the last century were the same for both glaciers (Oerlemans 2007). The difference in mass balance inferred from our data is in line with this finding: the long response time of Vadret da Morteratsch results in a low-lying glacier tongue that is too large for the current climate. Thus, this glacier exhibits disproportionately negative mass balance at low elevations. Vadret da Palü, in contrast, has a flat high-elevation accumulation area and a steep and shallow glacier tongue. Hence, the glacier reacts quickly to climate warming by getting rid of its tongue and retreating to higher elevations. The comparison of glacier dynamics (Oerlemans 2007) and mass balance for these neighbouring glaciers illustrates the impact of glacier shape on its reaction to climate warming. Treating glaciers as indicators for climate change is, thus, not straightforward, but is complicated by the geometrical characteristics of each individual glacier. The concept described above theoretically leads to high rates of mass loss for large and flat

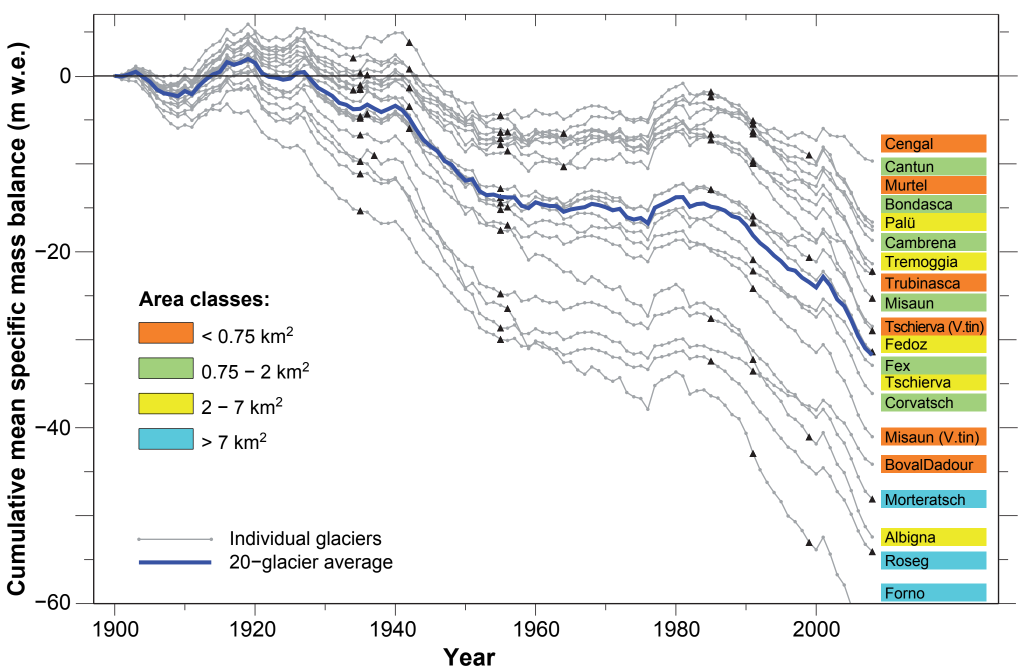

Fig. 7: Cumulative mass balance of the 20 investigated glaciers in the 20th century. Time series for the individual glaciers are displayed in grey; triangles indicate the dates of DEMs. The solid blue line represents the arithmetic average. Glacier names are given at the right hand side; colours indicate glacier size

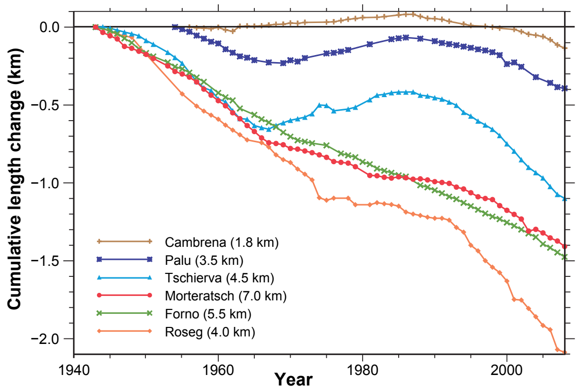

Fig. 8: Observed cumulative change in glacier length for 6 glaciers since the 1940s (GLACIOLOGICAL REPORTS 1881–2009). The glacier length in 2008 is given in brackets. Measurements of the first half of the 20th century are not shown

glaciers and to less negative mass balances for small and steep glaciers for the same anomalies in climatic forcing.

Differences in the rate of mass loss between the glaciers can also be explained by processes that affect either accumulation or melt for individual glaciers unequally. Although the investigated mountain group is relatively small in size, not all weather conditions favour snow accumulation for the entire glacier cluster in the same way. Large-scale atmospheric flow paths over the Alps showed strong variations over the 20th century leading to significant differences in the amount and the distribution of snow accumulation in Switzerland (Beniston 1997). Especially the glaciers of the Val Bregaglia, which strongly rely on high amounts of winter precipitation as well as avalanche-deposited snow, might be more sensitive to changes in the circulation pattern and thus wind direction than other ice masses. Positive and negative backcoupling mechanisms are expected with climate change, thus affecting individual glaciers differently in magnitude. Oerlemans et al. (2009) reported on increased dust-concentration in the ablation area of Vadret da Morteratsch leading to enhanced melt rates due to lower ice albedo. Conversely, many glaciers build up increasingly debris-covered tongues with glacier retreat, resulting in strongly reduced ice melt (Kayastha et al. 2000; Kellerer-Pirklbauer et al. 2008). The debris covered portion of Vadrec da l'Albigna, for example, increased from 16% in 1942 to 26% in 2003. Additionally, the supraglacial debris layer probably thickened, further reducing ice melt locally (Nakawo and Rana 1999). We expect this trend to persist over the next decades contributing to less negative mass balances and a slower reaction of Vadrec da l'Albigna to climate warming than for non-debris covered glaciers.

Correlations of decadal mean mass balance for large glacier samples with variables describing glacier geometry are generally weak; Paul and Haeberli (2008) obtained some dependency of the magnitude of glacier surface elevation change with glacier area and potential solar radiation. We divided the glacier areas of our 20-glacier sample into five groups corresponding to 20%-quantiles and evaluated the mean mass balance between 1900 and 2008 for each group (Fig. 9a). The relation between glacier area and mass balance is not straightforward; the group of the largest glaciers, however, shows by far the fastest mass loss. This corresponds to long response times and consequently slow adjustment of the glacier extent to changed climate conditions.

We define the volume ratio R_v that characterizes the distribution of the glacier's ice volume along its flowline. R_v is calculated by dividing the ice volume stored below the median glacier surface elevation by the volume stored above (Tab. 5). The ice thickness distribution is obtained from ITEM (Farinotti et al. 2009a). We find a clear relation between R_v and secular mass balance (Fig. 9b). Glaciers with high R_v, i.e. concentration of the ice volume in the ablation area, exhibit high rates of mass loss (e.g. Vadrec del Forno). Glaciers with low R_v, i.e. a steep and shallow glacier tongue and a flat and wide accumulation area, are characterized by less negative mass balances (e.g. Vadret da Palü). The volume ratio R_v seems to be a good indicator for estimating the mass balance reaction of glaciers to changed climate conditions.

Tab. 6: Comparison of five-decadal mean mass balances (1908-1958, 1958-2008) calculated using (i) the mass balance model constrained with ice volume changes and (ii) length change data (GLACIOLOGICAL REPORTS 1881-2009) according to Eq. 6 (Hoelzle et al. 2003)

Glacier	Mass balance model		Length change	
	$b_{1908-1958}$	$b_{1958-2008}$	$b_{1908-1958}$	$b_{1958-2008}$
Morteratsch	-0.44	-0.46	-0.32	-0.40
Roseg	-0.52	-0.48	-0.21	-0.41
Forno	-0.50	-0.72	-0.29	-0.36
Tschierva	-0.28	-0.33	-	-0.26
Palü	-0.13	-0.18	-0.22	-0.10
Cambrena	-0.18	-0.27	-	-0.04

The glaciers in the study area underwent short periods of mass gain in the 1910s and the late 1970s and showed rapid mass loss in the 1940s and since the mid-1980s (Fig. 7). This indicates that glacier retreat in the investigated region is driven by spatially coherent changes in meteorological variables to which the glaciers respond differently. For the investigation of long-term fluctuations and trends in the seasonal mass balance components, we analyzed the arithmetic 20-glacier average (Fig. 10). In general, long-term variations in glacier mass balance are due to changes in the melting conditions, well represented by the summer balance (Fig. 10). Long-term changes in the winter balance are small, although the year-to-year variability is considerable. However, periods of negative anomalies in summer balance often coincide with low winter balance, indicating that accumulation changes were at least partly responsible for rapid glacier mass loss in the 1940s and in the last decades (Fig. 10). Reduced accumulation in warm periods is related to the state of precipitation. For Swiss glaciers, Huss et al. (2009b) reported on a decrease in the fraction of solid precipitation of 12% since the 1970s. Furthermore, low winter accumulation enhances summer melting over an albedo feedback mechanism.

Extreme years – both with mass gain or loss – have strong impacts on glacier evolution. Our time series reveal some of these years, interestingly clustering in the first years of the 21st century. The year with the most negative summer balance is 2003 (Fig. 10), however, above average winter accumulation in south-eastern Switzerland has prevented the glaciers from undergoing very high mass losses. According to our evaluation, the mass balance year with the highest mass loss is 2006, characterized by low winter balance. In 1977 and 2001, the investigated glaciers showed very positive mass balances of +1.5 m w.e., due to winter accumulation being more than twice the long-term average.

In comparison to other studies addressing the glacier mass balance in the study region, we find similar results. Nemec et al. (2009) reported a cumulative mass balance for Vadret da Morteratsch of -46 m w.e. for the period 1865–2005. This result refers to an interpolation of mass balances calculated over the 1850 glacier extent and the current glacier geometry, and is thus difficult to directly compare to our cumulative mass balances calculated over annually updated glacier surfaces. The average glacier-wide mass balance of Vadret da Morteratsch for the period 1982–2002, which was determined by Klok and Oerlemans (2004) and based on an energy balance model, is -0.78 m w.e. a^{-1}. For the same time period, we obtained slightly less negative mass balances (-0.60 m w.e. a^{-1}). Hoelzle and Haeberli (1995) estimated the average mass balance for 7 glaciers contained in our sample between 1850 and 1973 as in the range of -0.27 to -0.52 m w.e. a^{-1}. For the same glaciers, we found a mean 1900–2008 mass balance of -0.33 m w.e. a^{-1}.

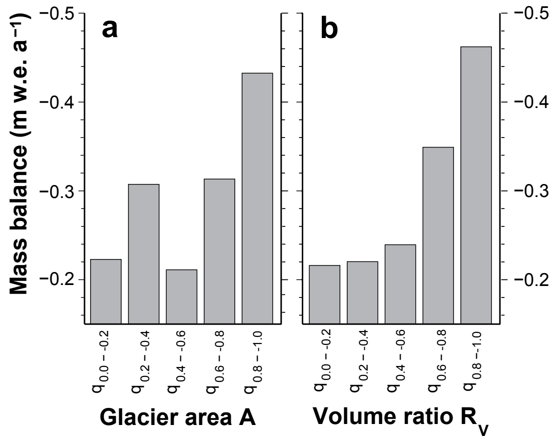

Fig. 9: Dependency of 1900-2008 mean mass balance on (a) glacier area and (b) the volume ratio R_V. Glaciers are grouped into five equal classes according to 20%-quantiles q. The bars show the mean mass balance of a glacier class

The differences in the 20th century mean ELA are considerable (Tab. 5) and range from 2250 m a.s.l. (Vadrec dal Cengal) to 3240 m a.s.l. (Vadrettin da Tschierva). This indicates that even within a small glacier cluster, accumulation and melting conditions can strongly differ. Low ELAs can either be explained by enhanced accumulation or by reduced melt, e.g. in shaded, north-exposed cirques. Analysis of the regional distribution of ELA over the 20th century shows that exposure is not dominant, but strong regional gradients in precipitation and snow redistribution processes are responsible for the relatively low-lying glacierization in the Val Bregaglia and the high ELAs around Piz Bernina.

The calculated 100-year trend in ELA rise is 15 m per decade and is significant according to the Mann-Kendall Test (Mann 1945; Kendall 1975). According to previous studies in the Alps (Greene et al. 1999; Maisch 2000) the ELA sensitivity to temperature rise is in the order of 150 m °C^{-1}. Our results are consistent with this number. The long-term fluctuations in the ELA are important and reached maxima around 1950 and over the last 20 years, and a local minimum between 1960 and 1980 (Fig. 11). We define ELA_0 as the ELA required to yield a balanced mass budget of the glacier. ELA_0

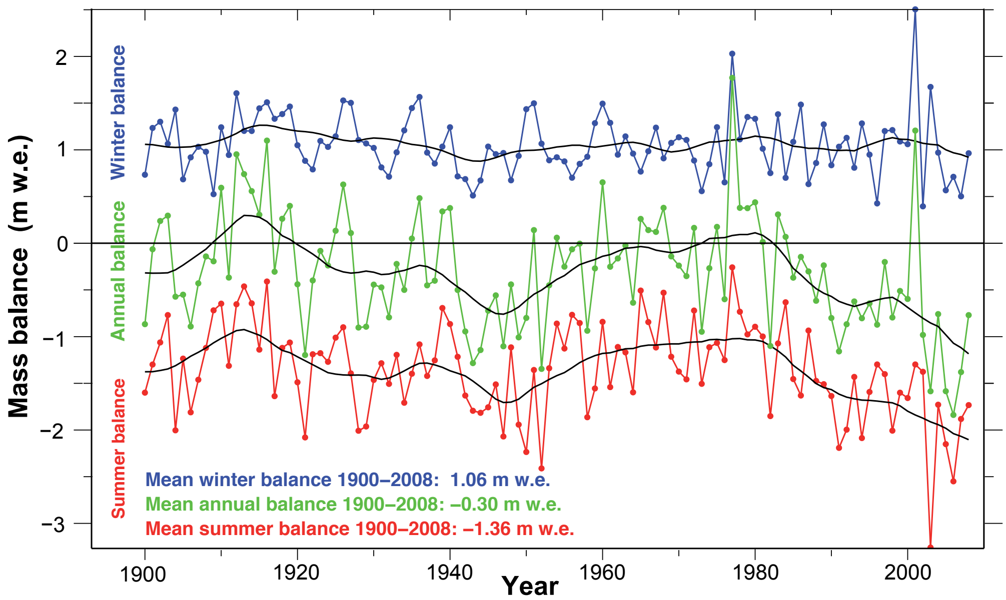

Fig. 10: Arithmetic average of the seasonal mass balance series of all investigated glaciers in 1900–2008. Annual data points of winter accumulation (positive), summer ablation (negative) and annual mass balance are low-pass filtered using 11-year running means

was determined for each year based on glacier extent and the Accumulation Area Ratio providing a balanced mass budget. ELA_0 increased steadily over the 20th century related to the retreat of the glacier towards higher elevations corresponding to a linear trend of 8 m per decade (Fig. 11). The comparison of time series of ELA and ELA_0 showed that the glaciers were almost always out of equilibrium conditions throughout the 20th century, except for two short periods in the 1910s and the 1960/70s. Differences in the long-term trend between ELA and ELA_0 indicate that the glaciers tend to go increasingly further from equilibrium conditions, i.e. they are not able to adjust their size as fast as the climate is changing.

4.2 Future perspectives for glacier extent and runoff

In order to provide perspectives for the future glacier changes in south-eastern Switzerland and to estimate potential impacts of glacier wastage on the hydrological cycle, we performed model runs using GERM for the 21st century based on climate scenarios. We assumed seasonal changes in air temperature and precipitation (Tab. 7) corresponding to the median of 16 Regional Climate Models (RCMs) within the PRUDENCE project (Christensen and Christensen 2007; Frei 2007). The models anticipated a significant increase in air temperature, especially pronounced in summer. Annual precipitation sums showed no large changes, however, more precipitation is expected in winter and less in summer (Tab. 7). Uncertainties in projections of future climate were high. This is both due to unknown future greenhouse gas emissions and backcoupling effects in the climate system that are insufficiently understood and implemented in the climate models. By using the median of a large model ensemble for the impact study, our scenario refers to a consensus about future climate evolution.

For each of the four analyzed drainage basins, we performed 20 transient calculations for the period 2009–2100 based on a random weather variability superimposed on the projected linear

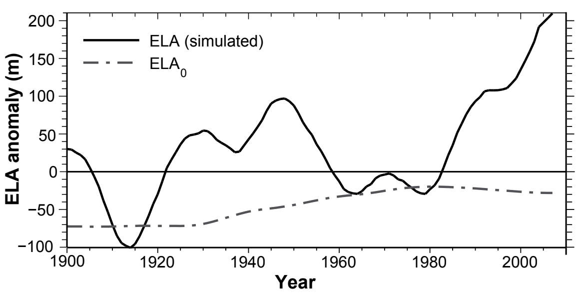

Fig. 11: Calculated anomaly in the equilibrium line altitude (deviation from 1961–1990) as average of the 8 investigated glaciers larger than 2 km². Smaller glaciers were not included because in warm years the ELA rises above the highest point of the glacier and is thus undefined. The dashed line represents the ELA that would yield a balanced mass bugdet, termed ELA_0. The lines represent 11-year running means

Tab. 7: Projected changes in seasonal temperature and precipitation for three time slices in the future relative to the year 1990. The values represent the median of 16 RCMs within the PRUDENCE project (Christensen and Christensen 2007; Frei 2007)

	Temp. change (°C)			Prec. change (%)		
Season	2030	2050	2070	2030	2050	2070
Winter	+0.9	+1.8	+2.5	+6	+11	+16
Spring	+0.9	+1.8	+2.6	-2	-4	-6
Summer	+1.5	+2.8	+4.0	-10	-19	-26
Autumn	+1.1	+2.2	+3.1	-2	-4	-5
Annual	+1.1	+2.2	+3.1	-2	-4	-5

trends in climate change (see Huss et al. 2008b for details). GERM yielded both the annual change in 3D glacier geometry and ice-covered area and calculated all components of the water balance in daily resolution.

The simulated retreat of the glaciers in the south-eastern Swiss Alps over the 21st century is strong. By 2050, we expect a decrease in total glacier area by 63% compared to 2003 (Tab. 5). Our results showed that very small glaciers will disappear within the next three decades (e.g. Vadret Boval Dadour, Vadrettin da Misaun), and glaciers with an area of currently 1–2 km² around 2050 (e.g. Vadret da Fedoz, Vadret dal Tremoggia). Some small glaciers in the Val Bregaglia, situated in north-exposed cirques, might last until the end of the 21st century (Vadrec da la Bondasca, Vadrec da la Trubinasca). This is intriguing, as their ELAs are partly as low as 2300 m a.s.l., an elevation, where one would not expect glaciers in a rapidly warming climate. We explain their resistivity to climate change with the strong dependency of their mass budget on winter accumulation and avalanches. Medium-sized glaciers are projected to withstand climate warming until about 2070 (e.g. Vadret da Roseg, Vadrec da l'Albigna) (Tab. 5).

According to our calculations, the largest glacier in the Region, Vadret da Morteratsch, will still be present, however, in strongly reduced size by 2100 (Fig. 12). By 2070, the ELA is expected to rise to 3500 m a.s.l. and the ice volume to have dropped to 10% relative to 2008 (Fig. 12). The AAR of Vadret da Morteratsch is around 40% throughout the entire 21st century indicating a strong and persistent imbalance of the glacier. An AAR of 58% would be required to yield a balanced mass budget. Our simple and widely applicable method to simulate future glacier geometry and extent does not assume the glacier to be in equilibrium with warming climate, but transiently keeps track of the ice volume. Taking into account these effects in future runoff projections is crucial for the management of water resources in alpine drainage basins.

In the glacierized drainage basins, we project strong changes in the components of the water balance. Although no significant trends in annual precipitation are expected (Tab. 7), the calculated

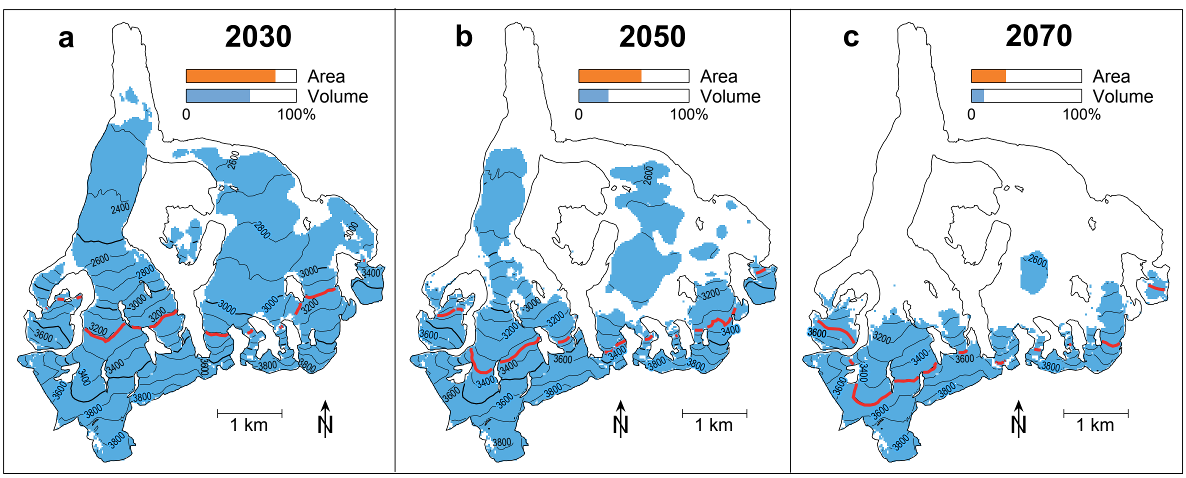

Fig. 12: Modelled future extent of Vadret da Morteratsch for (a) 2030, (b) 2050, and (c) 2070. Bars indicate the relative changes in glacier area and volume compared to 2008. The glacier outline in 2008 is shown and the solid red line refers to the 10-year average ELA for each time slice

Tab. 8: Evaluation of the water balance components. The values refer to the area-weighted average of the four investigated drainage basins (Tab. 2) and are presented according to the formulation of the water balance Q=P-E-ΔS, where Q is runoff, P is catchment precipitation, E is evapotranspiration and ΔS is the storage change. In glacierized catchments, ΔS is dominated by the changes in ice volume. The catchment glacierization (glac.) is given

Year	Q	P	E	ΔS	Glac.
		(mm a^{-1})			(%)
1961-90	1619	1732	192	-80	23.5
2030	1652	1715	284	-221	16.8
2050	1591	1745	351	-197	9.9
2070	1352	1712	411	-51	3.5
2090	1285	1746	469	-7	1.6

annual runoff over the 21st century shows considerable long-term variations (Tab. 8). Compared to the climatic normal period 1961–1990 we find a small increase in annual runoff (+2%) in 2030 (Fig. 13) which is due to the release of water from long-term glacier storage. For catchments with little vegetation and substantial glacierization the runoff maximum due to glacier melt is more pronounced (Fig. 13b). The subsequent runoff decrease is explained by higher evapotranspiration and the glaciers, strongly diminished in size, providing only small quantities of melt water (Tab. 8). We expect annual runoff volume from the four drainage basins to decrease by -23% by 2100. In catchments with a small portion of ice-covered and a high percentage of vegetated surfaces the changes in the water balance are dominated by the increase in evapotranspiration (Tab. 8). The modelling of this variable in high alpine environments and for future conditions is, however, relatively uncertain.

Changes in the runoff regime are expected to pose the major challenge for the water resource management in the 21st century. Our results show the gradual transition from a glacier-melt dominated to a snow-melt dominated hydrograph (Fig. 14). Whereas in a first phase until about 2050, an increase in summer runoff is expected due to strong ice melt and a fast reduction of glacier volume, we project a significant decrease in runoff in the months July and August for the second half of the century (Fig. 14). In a warmer climate, snow melt runoff starts earlier in the year, is more concentrated and has already terminated in summer. The glaciers – strongly reduced in size – can no longer provide ice melt runoff in the summer months, when there is the greatest need for water supply in dry alpine valleys. Higher evapotranspiration losses further increase the water shortage in summertime.

Our results indicate a 24% decrease in summer runoff (July–August) compared to 1961–1990 for the year 2050. By 2090, July–August runoff is expected to be diminished by even 63% (Fig. 14). Due to an earlier onset of the melting season, a significant increase in the spring runoff (April–May) by 54% is anticipated for 2050.

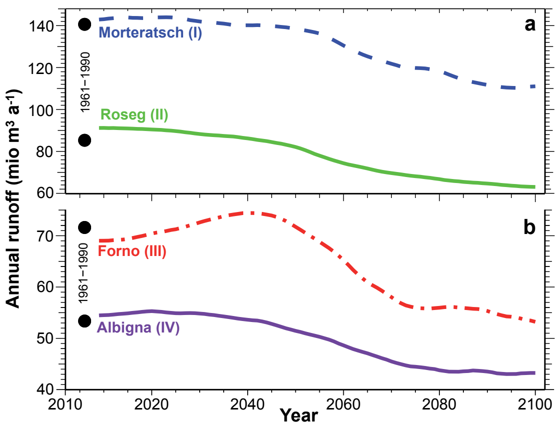

Fig. 13: Projected changes in annual discharge for all investigated drainage basins. Dots give the mean over the period 1961–1990

5 Conclusion

This study compiles the first set of long-term mass balance time series for all items in a glacier cluster. This allows the analysis of the differences in the response of adjacent ice masses to climatic warming. Our results are based on a simple mass balance model driven by daily meteorological data and constrained by various types of field measurements covering large parts of the 20th century. We provide seasonal glacier mass balance time series for 20 glaciers, different in size and geometry, in south-eastern Switzerland for the period 1900–2008. Strongly differing rates of glacier mass loss are mainly explained by the dynamic adjustment of the glacier to the current climate. The analysis of glacier change is complemented with estimates of the total ice volume, which is required for

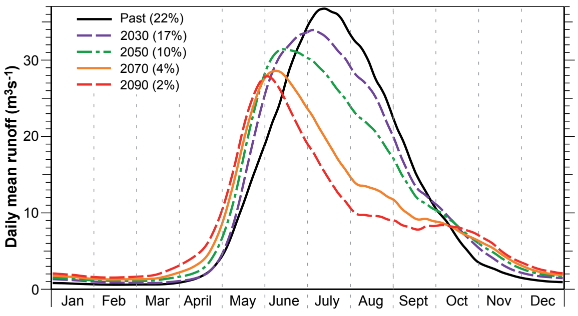

Fig. 14: Simulated changes in the runoff regime. The results of the four investigated catchments are summed up. The annual runoff cycle is shown for the climatic normal period (measurements) and for four time slices in the future. The glacierization is given in brackets

projections of glacier change into the future. Based on regional climate scenarios in seasonal resolution, we perform model runs until 2100 in order to provide perspectives for the change in glacier extent and the impact of glacier retreat on the runoff regime of glacierized drainage basins in south-eastern Switzerland. Glaciers in the study area are expected to retreat significantly over the next decades. Most of them will disappear in the second half of the 21st century. The hydrological cycle will be strongly affected by glacier retreat. According to our results, an initial increase in runoff due to strong reduction in glacier ice volume will be followed by a water shortage, particularly important during the summer months. Our analysis of glacier change over the last 100 years shows that understanding the response of glaciers to current atmospheric warming is complicated by many interactions of climate, glacier surface processes, ice dynamics and glacier geometry. Field data are the key to understanding these processes. However, for many regions, field measurements documenting long-term glacier changes are too sparse and thus do not clearly reveal the climate change impacts. Modelling is an essential tool for homogenizing and unifying these measurements and, hence, for increasing their value. This study does not present the results from a long-term glacier monitoring program, but is based on a compilation and re-analysis of existing data sets. Similar information is potentially available for a large number of glaciers in different mountain ranges and provides – in combination with short series of in-situ field measurements and modelling – an extended view of the response of mountain glaciers to 20th century climate warming. We recommend a strategy of combining various data sets to constrain models for the past and future change in mountain glacier extent, in order to estimate their contribution to global sea level rise, or for hydrological applications.

Acknowledgements

This work is supported by ETH Research Grant TH-17 06-1 and the BAFU project CCHydro. The meteorological data were recorded by MeteoSwiss. Swisstopo performed aerial photograph surveys and granted access to SwissImage and DHM25 level1. We thank CIAT for providing the SRTM data set. H. Bösch established DEMs from aerial photographs. Discharge data were provided by BAFU and Elektrizitätswerke Zürich. We are grateful to G. Gensler, J. Oerlemans, A. Palmer and previous researchers of the VAW-ETHZ for mass balance measurements. M. Funk is acknowledged for support and helpful discussions. Two anonymous reviewers commented on the manuscript.

References

Arendt, A. A.; Echelmeyer, K. A.; Harrison, W. D.; Lingle, C. S. and Valentine, V. B. (2002): Rapid wastage of Alaska glaciers and their contribution to rising sea level In: Science 297(5580), 382–386. DOI: 10.1126/science.1072497

Bahr, D. B.; Meier, M. F. and Peckham, S. D. (1997): The physical basis of glacier volume-area scaling. In: Journal of Geophysical Research 102 (B9), 20355–20362. DOI: 10.1029/97JB01696

Bauder, A.; Funk, M and Huss, M. (2007): Ice volume changes of selected glaciers in the Swiss Alps since the end of the 19th century. In: Annals of Glaciology 46, 145–149. DOI: 10.3189/172756407782871701

Begert, M.; Schlegel, T. and Kirchhofer, W. (2005): Homogeneous temperature and precipitation series of Switzerland from 1864 to 2000. In: International Journal of Climatology 25 (1), 65–80. DOI: 10.1002/joc.1118

Beniston, M. (1997): Variations of snow depth and duration in the Swiss Alps over the last 50 years: links to changes in large-scale climatic forcings. In: Climatic Change 36, 281–300. DOI: 10.1023/A:1005310214361

Berthier, E.; Arnaud, Y.; Vincent, C and Rémy, F. (2006): Biases of SRTM in high-mountain areas: implications for the monitoring of glacier volume changes. In: Geophysical Research Letters 33, L08502. DOI: 10.1029/2006GL025862

Braun, L.; Aellen, M.; Funk, M.; Hock, R; Rohrer, M.; Steinegger, U.; Kappenberger, G. and Mueller-Lemans, H. (1994): Measurement and simulation of high alpine water balance components in the Linth-Limmern head watershed (north-eastern Switzerland) . In: Zeitschrift für Gletscherkunde und Glazialgeologie 30, 161–185.

Burga, C. A. (1999): Vegetation development on the glacier forefield Morteratsch (Switzerland) . In: Applied Vegetation Science 2 (1), 17–24.

Bürki, R.; Elsasser, B. and Abegg, B. (2003): Climate change: impacts on the tourism industry in mountain areas. Proceedings of the 1st International Conference on Climate Change and Tourism, Djerba, 9–11 April 2003.

Chinn, T. J. (1996): New Zealand glacier responses to climate change of the past century. In: New Zealand Journal of Geology and Geophysics 39 (3), 415–428.

Christensen, J. H. and Christensen, O. B. (2007): A summary of the PRUDENCE model projections of changes in European climate by the end of this century. In: Climatic Change 81, 7–30. DOI: 10.1007/s10584-006-9210-7

Farinotti, D.; Huss, M.; Bauder, A.; Funk, M. and Truffer, M. (2009a): A method for estimating the ice volume and ice thickness distribution of alpine glaciers. In: Journal of Glaciology 55 (191), 422–430. DOI: 10.3189/002214309788816759

Farinotti, D.; Huss, M.; Bauder, A. and Funk, M. (2009b): An estimate of the glacier ice volume in the the Swiss Alps. In: Global and Planetary Change 68 (3), 225–231. DOI: 10.1016/j.gloplacha.2009.05.004

FIRNBERICHTE (1914–1978): Der Firnzuwachs 1913/14–1976/77 in einigen schweizerischen Firngebieten, no. 1-64 in Vierteljahresschrift der Naturforschenden Gesellschaft in Zürich.

Frei, C. (2007): Die Klimazukunft der Schweiz, Klimaänderung und die Schweiz 2050 – Erwartete Auswirkungen auf Umwelt, Gesellschaft und Wirtschaft, Beratendes Organ für Fragen der Klimaänderung (OcCC), 12–16, http://www.occc.ch.

Glaciological Reports (1881–2009): The Swiss glaciers, 1880–2004/05, No. 1-126, Yearbooks of the Cryospheric Commission of the Swiss Academy of Sciences (SCNAT), published since 1964 by Laboratory of Hydraulics, Hydrology and Glaciology (VAW) of ETH Zürich.

Greene, A. M.; Broecker, W. S. and Rind, D. (1999): Swiss glacier recession since the Little Ice Age: reconciliation with climate records. In: Geophysical Research Letters 26, 1909–1912. DOI: 10.1029/1999GL900380

Haeberli, W. and Hoelzle, M. (1995): Application of inventory data for estimating characteristics of and regional climate-change effects on mountain glaciers: a pilot study with the European Alps. In: Annals of Glaciology 21, 206–212.

Hamon, W. R. (1961): Estimating potential evapotranspiration. In: Journal of the Hydraulics Division 87 (HY3), 107–120.

Harrison, W. D.; Elsberg, D. H.; Cox L. H. and March, R. S. (2005): Different mass balances for climatic and hydrologic applications. In: Journal of Glaciology 51 (172), 176.

Hock, R. (1999): A distributed temperature-index ice- and snowmelt model including potential direct solar radiation. In: Journal of Glaciology, 45 (149), 101–111.

Hoelzle, M. and Haeberli, W. (1995): Simulating the effects of mean annual air-temperature changes on permafrost distribution and glacier size: an example from the Upper Engadin, Swiss Alps. In: Annals of Glaciology 21, 399–405.

Hoelzle, M.; Haeberli, W.; Dischl, M. and Peschke, W. (2003): Secular glacier mass balances derived from cumulative glacier length changes. In: Global and Planetary Change 36 (4), 295–306. DOI: 10.1016/S0921-8181(02)00223-0

Horton, P.; Schaefli, B.; Mezghani, A.; Hingray, B. and Musy, A. (2006): Assessment of climate-change impacts on alpine discharge regimes with climate model uncertainty. In: Hydrological Processes 20 (10), 2091–2109. DOI: 10.1002/hyp.6197

Huss, M.; Bauder, A. and Funk, M. (2009a): Homogenization of long-term mass balance time series. In: Annals of Glaciology 50 (50), 198–206. DOI: 10.3189/172756409787769627

Huss, M.; Funk, M. and Ohmura, A. (2009b): Strong Alpine glacier melt in the 1940s due to enhanced solar radiation. In: Geophysical Research Letters 36, L23501, DOI: 10.1029/2009GL040789

Huss, M.; Bauder, A.; Funk, M. and Hock, R. (2008a): Determination of the seasonal mass balance of four Alpine glaciers since 1865. In: Journal of Geophysical Research 113, F01015. DOI: 10.1029/2007JF000803

Huss, M.; Farinotti, D.; Bauder, A. and Funk, M. (2008b): Modelling runoff from highly glacierized alpine drainage basins in a changing climate. In: Hydrological Processes 22 (19), 3888–3902. DOI: 10.1002/hyp.7055

Huss, M.; Jouvet, G.; Farinotti, D. and Bauder, A. (2010): Future high-mountain hydrology: a new parameterization of glacier retreat. In: Hydrology and Earth System Sciences 14, 815-829. DOI: 10.5194/hess-14-815-2010

IPCC (2007): Climate change 2007. The scientific basis. Contributions of Working Group I to the Forth Assessment Report of the Intergovernmental Panel on Climate Change, WMO/UNEP.

Jarvis, J.; Reuter, H. I.; Nelson, A. and Guevara, E. (2008): Hole-filled SRTM for the globe Version 4, available from the CGIAR-CSI SRTM 90 m Database.

Jóhannesson, T.; Raymond, C. and Waddington, E. (1989): Time-scale for adjustment of glaciers to changes in mass balance. In: Journal of Glaciology 35 (121), 355–369.

Jouvet, G.; Huss, M.; Blatter, H.; Picasso, M. and Rappaz, J. (2009): Numerical simulation of Rhonegletscher from 1874 to 2100. In: Journal of Computational Physics 228 (17), 6426–6439. DOI: 10.1016/j.jcp.2009.05.033

Kaser, G.; Cogley, J. G.; Dyurgerov, M. B.; Meier, M. F. and Ohmura, A. (2006): Mass balance of glaciers and ice caps: consensus estimates for 1961–2004. In: Geophysical Research Letters 33 (19), L19501. DOI: 10.1029/2006GL027511

Kayastha, R. B.; Takeuchi, Y.; Nakawo, M. and Ageta, Y. (2000): Practical prediction of ice melting beneath various thickness of debris cover on Khumbu Glacier, Nepal, using a positive degree-day factor, Debris-Covered Glaciers. IAHS 264, 71–82.

Kellerer-Pirklbauer, A.; Lieb, G. K.; Avian, M. and Gspurnin, J. (2008): The response of partially debris-covered valley glaciers to climate change: The example of the Pasterze glacier (Austria) in the period 1964 to 2006. In: Geografiska Annaler 90, 269–285. DOI: 10.1111/j.1468-0459.2008.00345.x

Kendall, M. G. (1975): Rank correlation methods. London.

Klok, E. J. and Oerlemans, J. (2002): Model study of the spatial distribution of the energy and mass balance of Morteratschgletscher, Switzerland. In: Journal of Glaciology 48 (163), 505–518.

– (2004): Modelled climate sensitivity of the mass balance of Morteratschgletscher and its dependence on albedo parameterization. In: International Journal of Climatology 23, 231–245. DOI: 10.1002/joc.994

Kuhn, M.; Markel, G.; Kaser, G.; Nickus, U.; Obleitner, F. and Schneider, H. (1985): Fluctuations of climate and mass balances: different responses of two adjacent glaciers. In: Zeitschrift für Gletscherkunde und Glazialgeologie 21 (1), 409–416.

Lehning, M.; Loewe, H; Ryser, M. and Raderschall, N. (2008): Inhomogeneous precipitation distribution and snow transport in steep terrain. In: Water Resources Research 44 W07404. DOI: 10.1029/2007WR006545

Machguth, H.; Purves, R. S.; Oerlemans, J.; Hoelzle, M. and Paul, F. (2008): Exploring uncertainty in glacier mass balance modelling with Monte Carlo simulation. In: The Cryosphere 2, 191–204. DOI: 10.5194/tc-2-191-2008

Maisch, M. (2000): The long-term signal of climate change in the Swiss Alps: glacier retreat since the end of the Little Ice Age and future ice decay scenarios. In: Geogr. Fis. Dinam. Quat. 23, 139–151.

Mann, H. B. (1945): Nonparametric tests against trend. In: Econometrika 13, 245–259.

Nakawo, M. and Rana, B. (1999): Estimate of ablation rate of glacier ice under a supraglacial debris layer. In: Geografiska Annaler 81 (4), 695–701. DOI: 10.1111/j.0435-3676.1999.00097.x

Nash, J. E. and Sutcliffe, J. V. (1970): River flow forecasting through conceptual models. In: Journal of Hydrology 10 (3), 282–290. DOI: 10.1016/0022-1694(70)90255-6

Nemec, J.; Huybrechts, P.; Rybak, O. and Oerlemans, J. (2009): Reconstruction of the annual balance of Vadret da Morteratsch, Switzerland, since 1865. In: Annals of Glaciology 50 (50), 126–134. DOI: 10.3189/172756409787769609

Nye, J. F. (1960): The response of glaciers and ice-sheets to seasonal and climatic changes. In: Proceedings of the Royal Society of London, Ser. A 256 (1287), 559–584.

Oerlemans, J. (1994): Quantifying global warming from the retreat of glaciers. In: Science 264, 243–245. DOI: 10.1126/science.264.5156.243

– (2000): Analyis of a three-year meteorological record from the ablation zone of the Morteratschgletscher, Switzerland: energy and mass balance. In: Journal of Glaciology 46 (155), 571–579. DOI: 10.3189/172756500781832657

– (2007): Estimating response times of Vadret da Morteratsch, Vadret da Palü, Briksdalsbreen and Nigardsbreen from their length records. In: Journal of Glaciology 53 (182), 357–362. DOI: 10.3189/002214307783258387

Oerlemans, J. and Klok, E. J. (2002): Energy Balance of a Glacier Surface: Analysis of Automatic Weather Station Data from the Morteratschgletscher, Switzerland. In: Arctic, Antarctic and Alpine Research 34 (4), 477–485.

Oerlemans, J.; Giessen, R. H. and van den Broeke, M. R. (2009): Retreating alpine glaciers: increased melt rates due to accumulation of dust (Vadret da Morteratsch, Switzerland) . In: Journal of Glaciology 55 (192), 729–736. DOI: 10.3189/002214309789470969

Ohmura, A.; Bauder, A.; Müller, H. and Kappenberger, G. (2007): Long-term change of mass balance and the role of radiation. In: Annals of Glaciology 46, 367–374. DOI: 10.3189/172756407782871297

Palmer, A. S.; Schwikowski, M. and Gaeggeler, H. W. (2003): A subseasonal trace chemical ice core record from Piz Zupo, Swiss Alps. In: Geophysical Research Abstracts 5 (01331).

Paterson, W. S. B. (1994): The physics of glaciers. New York.

Paul, F. (2008): Calculation of glacier elevation changes with SRTM: is there an elevation-dependent bias? In: Journal of Glaciology 54 (188), 945–946. DOI: 10.3189/002214308787779960

Paul, F. and Haeberli, W. (2008): Spatial variability of glacier elevation changes in the Swiss Alps obtained from two digital elevation models. In: Geophysical Research Letters 35, L21502. DOI: 10.1029/2008GL034718

Pellicciotti, F.; Brock, B.; Strasser, U.; Burlando, P.; Funk, M. and Corripio, J. (2005): An enhanced temperature-incex glacier melt model including the shortwave radiation balance: development and testing for Haut Glacier d'Arolla, Switzerland. In: Journal of Glaciology 51 (175), 573–587. DOI: 10.3189/172756505781829124

Raper, S. C. B. and Braithwaite, R. J. (2006): Low sea level rise projections from mountain glaciers and icecaps under global warming. In: Nature 439, 311–313. DOI: 10.1038/nature04448

Richardson, S. D. and Reynolds, J. M. (2000): An overview of glacial hazards in the Himalayas. In: Quaternary International 65–66, 31–47. DOI: 10.1016/S1040-6182(99)00035-X

Sapiano, J.; Harrison, W. D. and Echelmeyer, K. A. (1998): Elevation, volume and terminus changes of nine glaciers in North America. In: Journal of Glaciology 44 (146), 119–135.

Schaefli, B.; Hingray, B. and Musy, A. (2007): Climate change and hydropower production in the Swiss Alps: quantification of potential impacts and related modelling uncertainties. In: Hydrology and Earth System Sciences 11 (3), 1191–1205. DOI: 10.5194/hess-11-1191-2007

Schwarb, M.; Daly, C.; Frei; C. and Schaer, C. (2001): Mean annual and seasonal precipitation throughout the European Alps 1971–1990. Hydrological Atlas of Switzerland, plates 2.6, 2.7.

Stahl, K.; Moore, R. D.; Shea, J. M.; Hutchinson, D. and Cannon, A. J. (2008): Coupled modelling of glacier and streamflow response to future climate scenarios. In: Water Resources Research 44, W02422. DOI: 10.1029/2007WR005956

Steiner, D.; Pauling, A.; Nussbaumer, S. U.; Nesje, A.; Luterbacher, J.; Wanner, H. and Zumbühl, H. J. (2008): Sensitivity of European glaciers to precipitation and temperature – two case studies. In: Climatic Change 90 (4), 413–441. DOI: 10.1007/s10584-008-9393-1

Theurillat, J.-P. and Guisan, A. (2001): Potential impact of climate change on vegetation in the european alps: a review. In: Climatic Change 50, 77–109. DOI: 10.1023/A:1010632015572

Thibert, E.; Blanc, R.; Vincent, C. and Eckert, N. (2008): Glaciological and volumetric mass balance measurements error analysis over 51 years for Glacier de Sarennes, French Alps. In: Journal of Glaciology 54 (186), 522–532. DOI: 10.3189/002214308785837093

VAW (1962): Hydrologisch-glaziologische Untersuchungen in den Einzugsgebieten des Albigna- und Forngletschers. Report no.70.2 (P. Kasser, unpublished), Versuchsanstalt für Wasserbau, Hydrologie und Glaziologie der ETH Zürich.

Vincent, C. (2002): Influence of climate change over the 20th Century on four French glacier mass balances. In: Journal of Geophysical Research 107 (4375), D19. DOI: 10.1029/2001JD000832

Vincent, C.; Kappenberger, G.; Valla, F.; Bauder, A.; Funk, M. and Le Meur, E. (2004): Ice ablation as evidence of climate change in the Alps over the 20th century. In: Journal of Geophysical Research 109 (D10), D10104. DOI: 10.1029/2003JD003857

Zemp, M.; Hoelzle, M. and Haeberli, W. (2009): Six decades of glacier mass-balance observations: a review of the worldwide monitoring network. In: Annals of Glaciology 50 (50), 101–111. DOI: 10.3189/172756409787769591

Zemp, M.; Haeberli, W.; Hoelzle, M. and Paul, F. (2006): Alpine glaciers to disappear within decades? In: Geophysical Research Letters 33 (13), L13504. DOI: 10.1029/2006GL026319

Zierl, B. and Bugmann, H. (2005): Global change impacts on hydrological processes in Alpine catchments. In: Water Resources Research 41, W02028. DOI: 10.1029/2004WR003447

Authors

Dr. Matthias Huss
Department of Geosciences
University of Fribourg
Chemin du Musée 4
1700 Fribourg
Switzerland
matthias.huss@unifr.ch

Stephanie Usselmann
Daniel Farinotti
Dr. Andreas Bauder
Laboratory of Hydraulics, Hydrology and Glaciology (VAW)
ETH Zurich
Gloriastrasse 37-39
8092 Zurich
Switzerland
usselmann@vaw.baug.ethz.ch
farinotti@vaw.baug.ethz.ch
bauder@vaw.baug.ethz.ch.